

# Raman microscopy of prehistoric paintings in French megalithic monuments

Antonio Hernanz,<sup>a\*</sup> Mercedes Iriarte,<sup>a</sup> Primitiva Bueno-Ramírez,<sup>b</sup> Rodrigo de Balbín-Behrmann,<sup>b</sup> Jose M. Gavira-Vallejo,<sup>a</sup> Delia Calderón-Saturio,<sup>a</sup> Luc Laporte,<sup>c</sup> Rosa Barroso-Bermejo,<sup>b</sup> Philippe Gouezin,<sup>c</sup> Angel Maroto-Valiente,<sup>d</sup> Laure Salanova,<sup>e</sup> Gerard Benetau-Douillard<sup>f</sup> and Emmanuel Mens<sup>g</sup>



Remains of pictorial decorations in a series of six representative megalithic monuments of Brittany (France) and two French stelae have been studied by micro-Raman spectroscopy for the first time. Fungal colonies on the painted orthostats made it difficult to obtain *in situ* Raman spectra of the paint components. Nevertheless, paint micro-specimens studied in the laboratory by micro-Raman spectroscopy, X-ray photoelectron spectroscopy and scanning electronic microscopy combined with energy dispersive X-ray spectroscopy have made possible to characterise the materials present. The minerals  $\alpha$ -quartz, albite, microcline, muscovite, phlogopite, celadonite, beryl and anatase have been identified in the granitic rocks supporting the paintings, while dolomite and calcite are dominant in the calcareous rocky substrata. Haematite is the main component of the red pictographs, whereas amorphous carbon and manganese oxides/oxihydroxides have been used in the black ones. Calcite, gypsum and amorphous carbon have been detected as additional components of the paint in some cases. Contamination with modern tracing materials (polystyrene and  $\epsilon$ -copper-phthalocyanine blue) has been detected in several cases. The presence of pigments as decorative elements in megalithic monuments of Western France and its possible relation with those of the Iberian Peninsula create interesting expectations for the knowledge of the European megalithic culture. Copyright © 2015 John Wiley & Sons, Ltd.

Additional supporting information may be found in the online version of this article at the publisher's web site.

**Keywords:** portable Raman microscopy; SEM/EDX; XPS; megalithic monuments; prehistoric paintings

## Introduction

Western France megalithism represents the biggest group of decorated monuments found within the Atlantic façade. Megalithic art was characterised as a discipline based on the data obtained in this area. Along this process, engraving was defined to be the only identifiable intervention. The presence of pigments as decorative elements was only admitted for a scarce number of sites located in northwestern Iberian Peninsula. Nevertheless, new techniques have led to demonstrate the abundance of pigments in megalithic monuments around the Iberian Peninsula. The knowledge of the building process, the maintenance and the use of megaliths are benefited by the increasing possibilities for characterising and dating pigments.<sup>[1,2]</sup> Thereby, the more pigments are found within the megaliths record from such a representative area as Brittany, the deeper impact on the interpretation of the Atlantic façade's symbolic world, and the wider our understanding becomes.<sup>[3,4]</sup> Raman spectroscopy with complementary techniques is a powerful tool to identify prehistoric pigments.<sup>[5–12]</sup> Hence, it is very motivating to investigate vestiges of pictorial decorations in this fundamental megalithic area for the first time. Six representative megalithic monuments and two stelae from Western France have been selected for this purpose, Fig. S1 (Supporting Information). Raman spectra from a large number of points may be obtained *in situ* with portable micro-Raman spectroscopy ( $\mu$ -RS) instruments, thereby avoiding numerous extractions of specimens.<sup>[8,10,12,13]</sup> Orthostats

with possible rests of paintings are usually in tumulus chambers without light and wind, two advantages for *in situ*  $\mu$ -RS.<sup>[12]</sup> Possible

\* Correspondence to: Antonio Hernanz, Departamento de Ciencias y Técnicas Fisicoquímicas, Universidad Nacional de Educación a Distancia, Paseo Senda del Rey 9, E-28040 Madrid, Spain.  
E-mail: ahernanz@ccia.uned.es

a Departamento de Ciencias y Técnicas Fisicoquímicas, Facultad de Ciencias, Universidad Nacional de Educación a Distancia, Paseo Senda del Rey 9, E-28040 Madrid, Spain

b Departamento de Historia y Filosofía, Facultad de Filosofía y Letras, Universidad de Alcalá de Henares, Colegios 2, E-28801 Alcalá de Henares, Madrid, Spain

c UMR 6566-CReAAH, Université Rennes 1, Campus de Beaulieu, 35042 Rennes Cedex, France

d Departamento de Química Inorgánica y Química Técnica, Facultad de Ciencias, Universidad Nacional de Educación a Distancia, Paseo Senda del Rey 9, E-28040 Madrid, Spain

e UMR 7401, Université Paris Ouest Nanterre La Défense, 21 allée de l'Université, 92023 Nanterre, France

f Laboratoire d'Archéologie et d'Anthropologie Sociale, Z. A. Les Guignerries, 85320 La Bretonnière-La Claye, France

g Laboratoire TRACES, UMR5608, Université Toulouse Jean Jaurés, Maison de la Recherche 5, allée Antonio Machado, 31058 Toulouse Cedex 9, France

pictorial materials have been analysed by *in situ*  $\mu$ -RS. Some micro-specimens from carefully selected points have been removed in order to be studied in the laboratory by  $\mu$ -RS, scanning electronic microscopy combined with energy dispersive X-ray spectroscopy (SEM/EDX) and X-ray photoelectron spectroscopy (XPS). Possible pigment characterisation and dating<sup>[14,15]</sup> contribute invaluable insight to the construction, preservation and use of the megaliths. To assess the presence of painted decorations in such a characteristic megalithic region as Brittany is an effort with evident consequences for the knowledge of the megalithic culture in Atlantic Europe.

### Archaeological background

The chosen megaliths are the most representative within the classic sequence of Brittany: chambers A and H from Barnenez tumulus (Plouezoc'h, Finistère), the gallery of Goërem (Gâvres, Morbihan), the monuments from Dissignac (Saint-Nazaire, Loire-Atlantique) or the dolmens integrated inside the tumulus of Mont-Saint-Michel (Carnac, Morbihan).<sup>[16]</sup> Another group of monuments has been chosen because of their current preservation state: Mané Rutual (Locmariaquer, Morbihan) and Mané Kerioned B (Carnac, Morbihan). Although they are open to the public and have been vandalised, it is still feasible to restore some of the decorations. The oldest megalithic monuments from Brittany are dated around the fifth millennia cal BC including Barnenez tumulus,<sup>[17]</sup> Mont-Saint-Michel and other earlier evidences. The stelae from the megalithic quarry of L'Hirondelle (Bois de Fourgon, Avrillé, Vendée)<sup>[18]</sup> and the one from the Neolithic collective grave from Saint-Claude (Bury, Oise)<sup>[19]</sup> are included within this timeframe as well. The selected stelae describe the link between anthropomorphic figures and the northwestern Atlantic contexts, on one hand. On the other hand, L'Hirondelle's site is an outdoor area that proves the presence of open-air decorated complexes way beyond the Mediterranean area.

### Experimental

Descriptions of the instruments used for the  $\mu$ -RS, SEM/EDS and XPS studies, as well as the protocol used for micro-specimen extractions, have been given elsewhere.<sup>[11,12,20]</sup> Specific experimental details of this work are reported here. *In situ*  $\mu$ -RS spectra have been obtained with a BWTEK innoRam 785H portable Raman microscope. An optical fibre cable connects the spectrometer to a handheld probe head with 10 $\times$  magnification and alternatively to a microscope/video camera set with 20 $\times$  objective lens supported on an XYZ focusing system, Fig. S2 (Supporting Information). The laser line at 785 nm has been used for Raman excitation with powers between 3 and 16 mW measured at the focus position. Càrol's cap<sup>[12]</sup> was mounted over the probe head or the objective to avoid sunlight or other external radiation entering in the spectrometer. The spectral range from 65 to 2500  $\text{cm}^{-1}$  (Stokes) was recorded with a spectral resolution  $s \sim 3.5 \text{ cm}^{-1}$ . Integration times of 2–3 s and 36 spectral accumulations have been used to achieve an acceptable signal-to-noise ratio. Wavenumber shift calibration of this spectrometer was accomplished with Hg-I lines, 4-acetamidophenol, naphthalene and sulfur standards<sup>[21]</sup> over the range 150–1800  $\text{cm}^{-1}$ . This resulted in a wavenumber mean deviation of  $\Delta v_{\text{cal}} - \Delta v_{\text{obs}} = -0.01 \pm 0.05 \text{ cm}^{-1}$  ( $t_{\text{Student}}$  95%).<sup>[21]</sup> The location of some of the points that have been analysed *in situ* is indicated (red circles) in Figs S3–S23 (Supporting Information). Micro-specimens (size  $\leq 1 \text{ mm}^2$ ) of the pigmented areas were extracted from the different sites for additional laboratory analyses;

the points of these extractions are indicated with white circles in Figs S3–S23 (Supporting Information). Microphotographs of the points analysed *in situ* and those used for the extractions were obtained with a portable microscope Lumos X-Loupe G20-FA11-00 equipped with a digital camera Canon IXUS 120IS using 10 $\times$  magnification. The  $\mu$ -RS study of the extracted specimens has been carried out with a Jobin Yvon LabRam-IR HR-800 confocal Raman spectrograph coupled to an Olympus BX41 microscope. The 632.8 nm line of a He/Ne laser has been used for Raman excitation with powers of 764 and 745  $\mu\text{W}$  (100 $\times$  and 50 $\times$  LWD objective lenses, respectively) measured at the sample position. The average spectral resolution in the Raman shift range of 100–1700  $\text{cm}^{-1}$  was 1  $\text{cm}^{-1}$  (focal length 800 mm, grating 1800 grooves/mm and confocal pinhole 100  $\mu\text{m}$ ). These conditions involved a lateral resolving power of  $\sim 1\text{--}2 \mu\text{m}$  (100 $\times$  objective lens) and  $\sim 5 \mu\text{m}$  (50 $\times$  LWD objective lens) at the specimen. The depth of laser focus is 0.34 and 1.10  $\mu\text{m}$  for the 100 $\times$  and 50 $\times$  LWD objective lenses, respectively. An integration time of between 2 and 30 s and up to 64 accumulations have been used to achieve an acceptable signal-to-noise ratio. Wavenumber shift calibration applying the method indicated previously<sup>[21]</sup> over the range 150–3100  $\text{cm}^{-1}$  resulted in a wavenumber mean deviation of  $\Delta v_{\text{cal}} - \Delta v_{\text{obs}} = 2.01 \pm 1.79 \text{ cm}^{-1}$  ( $t_{\text{Student}}$  95%). Spectral smoothing was not applied to the observed spectra. The software package GRAMS/AI v.7.00 (Thermo Electron Corporation, Salem, NH, USA) has been used to correct the spectral background of fluorescence radiation, as well as to assist in determining the wavenumber of the peaks. Halogen lamp spectra from a cold light source Euromex LE.5210 have been used for spectral background corrections.

X-ray microanalyses of the extracted specimens have been carried out using an EDS spectrometer Rontec Xflash Detector 3001 with the Be window removed and coupled to a Hitachi S-3000 N scanning electron microscope (Everhart–Thornley detector of secondary electrons) with an operating resolution of 3 nm (working distance 4 mm, voltage applied 30 kV and pressure  $1.5 \times 10^{-3}$  Pa).

X-ray photoelectron spectroscopy spectra have been recorded with an Omicron spectrometer equipped with an EA-125 hemispherical electron multichannel analyser and unmonochromatised Al K $\alpha$  X-ray source with a radiation energy of 1486.6 eV. The specimens have been pressed into small pellets of  $\sim 5\text{--}15$  mm diameter. Nevertheless, because of their solid consistency, the surface with pictorial materials of the specimens 6 and 1, from the chamber H of Barnenez tumulus and Mané Rutual monument respectively, have been studied with no physical treatments prior to their analyses. The resulting spectral data have been analysed using the CASA XPS software and RSF database for peak fitting and Shirley background correction. The binding energy has been referenced to the adventitious C 1 s peak at 285 eV.

### Results and discussions

Pictorial materials from eight French megalithic sites are considered next. The results obtained are summarised in Table 1.

#### Barnenez tumulus

Initial studies on the chamber H of this monument,<sup>[4,16]</sup> Figs S4–S6 (Supporting Information), revealed that the main components of its orthostats were  $\alpha$ -quartz, albite and muscovite; all of them are common components of granitic rocks. The SEM/EDS spectra of the specimens 1, 2 and 6 from this chamber reveal a significant content of Mn, Fig. S24 (Supporting Information). The presence of

**Table 1.** Components identified in the rock and paintings in eight French megaliths

Megalith	Specimen	Rock components		Paint components	
		Primary phase	Secondary phases	Primary phases	Secondary phases
Barnenez tumulus chamber H, orth. C	1, 2, 6	<i><math>\alpha</math>-Quartz</i>	Albite, muscovite	a.c., Manganese oxides/oxyhydroxides (bixbyite, haussmanite, pyrochroite, todorokite, manganosite, cryptomelane)	Calcite, haematite, tracing materials <sup>a</sup>
	3	<i><math>\alpha</math>-Quartz</i>	Albite, muscovite, phlogopite, beryl	Haematite	Gypsum, a.c., calcite, tracing materials <sup>a</sup>
	4	<i><math>\alpha</math>-Quartz</i>	Albite, muscovite	Haematite	Gypsum, a.c., calcite
	5	<i><math>\alpha</math>-Quartz</i>	Albite, muscovite	a.c. (Charcoal)	
	1, 8	<i>Albite</i>	<i><math>\alpha</math>-Quartz</i>	—	—
	2–4	<i><math>\alpha</math>-Quartz</i>	<i>Albite</i>	—	—
	5, 7	<i>Fungi</i>	—	—	—
	6, 10–13	<i>Fungi</i>	—	—	—
	9, 14	<i><math>\alpha</math>-Quartz</i>	—	—	—
	Barnenez tumulus chamber A, entrance orth.	1	<i><math>\alpha</math>-Quartz</i>	Albite, muscovite	Goethite
2		<i><math>\alpha</math>-Quartz</i>	Albite, muscovite	Goethite	
Gallery of Goërem	1–4	<i><math>\alpha</math>-Quartz</i>	Albite, muscovite, anatase	a.c.	—
	5	<i><math>\alpha</math>-Quartz</i>	Albite, muscovite, anatase	—	—
Mont-Saint-Michel tumulus, Dolmen 1	1	<i><math>\alpha</math>-Quartz</i>	Albite, muscovite, celadonite	Haematite	—
Dolmen 2	1	<i><math>\alpha</math>-Quartz</i>	Albite, muscovite, celadonite	a.c.	—
Dolmen 3	1	<i><math>\alpha</math>-Quartz</i>	Albite, muscovite, celadonite	a.c.	—
	2	<i><math>\alpha</math>-Quartz</i>	Albite, muscovite, celadonite	a.c., Haematite	—
	3, 4	<i><math>\alpha</math>-Quartz</i>	Albite, muscovite, celadonite	a.c.	—
	1	<i>Fungi</i>	<i><math>\alpha</math>-Quartz</i>	—	—
	2, 3	<i><math>\alpha</math>-Quartz</i>	—	—	—
	4–6	<i>Fungi</i>	—	—	—
Dissignac tumulus	1–7, 10, 11	<i>Fungi</i>	—	—	—
	8, 9	<i>Fungi</i>	<i><math>\alpha</math>-Quartz</i>	—	—
Mané Rutual dolmen	1	<i><math>\alpha</math>-Quartz</i>	—	Haematite	—
Mané Kerioned B dolmen	1	<i><math>\alpha</math>-Quartz</i>	Albite, muscovite	Haematite	a.c.
L'Hirondelle stela	1	Dolomite	Calcite	Haematite	a.c.
	2	Dolomite	Calcite	Goethite	a.c.
Bury stela	1	<i><math>\alpha</math>-Quartz</i>	—	—	—
	2	<i><math>\alpha</math>-Quartz</i>	—	a.c.	Calcite
	3	<i><math>\alpha</math>-Quartz</i>	Microcline, anatase	Haematite	—
	4	<i><math>\alpha</math>-Quartz</i>	—	a.c.	Calcite

a.c., amorphous carbon; orth., orthostat.

<sup>a</sup>polystyrene,  $\epsilon$ -copper-phthalocyanine blue and a saturated organic compound.

The components are given in order of abundance. Results for points analysed *in situ* by micro-Raman spectroscopy are indicated in italics.

Mn in these specimens has also been identified by XPS, Table S1 (Supporting information). Raman spectra of these specimens of black paint from the chamber H, Fig. 1A, show broad bands in the typical spectral region of Mn–O and Mn–OH bending and stretching vibrations (450–800 cm<sup>-1</sup>).<sup>[22–30]</sup> This suggests the presence of Mn oxides (Mn<sub>x</sub>O<sub>y</sub>) and oxyhydroxides (Mn<sub>x</sub>O<sub>y</sub>(OH)<sub>z</sub>). The identification of manganese compounds used in rock art by Raman spectroscopy is frequently difficult.<sup>[6,10,31–33]</sup> No clear Raman signature is often obtained probably because of the low Raman activity of the manganese-based pigments, low crystallinity<sup>[10]</sup> and high degree of chemical heterogeneity (different manganese compounds can be present simultaneously even at the microscopic level).<sup>[33]</sup> Manganese oxides/hydroxides may suffer thermal alterations even at low laser power values,<sup>[23–25,29,31,34]</sup> manganese exists in several oxidation states and exhibits many hydro-oxides

modifications, many of them being non-stoichiometric and disordered compounds.<sup>[35]</sup> Furthermore, changes in the Raman spectra of manganese minerals have been related to their crystal size,<sup>[36]</sup> and significant wavenumber variations of the Raman bands of cryptomelane, a manganese mineral used in rock art, have been related to variations in the composition of this mineral.<sup>[37]</sup> Consequently, only a tentative assignment of the representative Raman spectra shown in Fig. 1A is considered next. A very broad and asymmetric band with a maximum at 643 cm<sup>-1</sup>, Fig. 1A(a), is frequently observed in these specimens. A study on Magdalenian pigments from Grottes de la Garenne (France) assigned this band to cryptomelane,<sup>[37]</sup> in disagreement with UV Raman data for this mineral.<sup>[25]</sup> This band could also be assigned to todorokite,<sup>[24,38]</sup> pyrochroite<sup>[4,38]</sup> and manganosite.<sup>[22]</sup> A multi-peak Lorentzian curve fitting of a similar band observed in black drawings from an

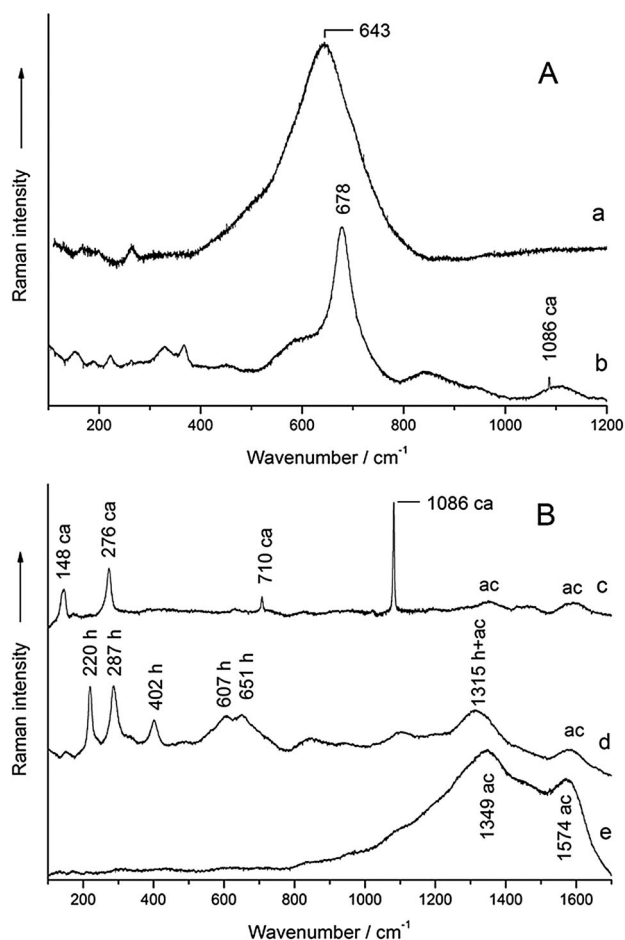


**Figure 1.** Representative micro-Raman spectroscopy spectra obtained from specimens 1, 2 and 6 of the black paint used in the chamber H of Barnenez tumulus, Fig. S6 (Supporting Information). A: spectra (a) and (b) suggest the presence of Mn oxides/oxyhydroxides. B: additional components. ac, amorphous carbon; ca, calcite; h, haematite.

Eritrean rock art site suggested the presence of bixbyite and hausmanite.<sup>[32]</sup> In fact, the large half bandwidth of the band indicates a not well-crystallised material; this makes its assignment difficult. Moreover, the asymmetry of the band admits several components to describe the spectral profile. Hence, a mixture of different Mn oxides/oxyhydroxides is possible. Wüstite, a non-stoichiometric iron oxide ( $\text{Fe}_{0.84}\text{O}-\text{Fe}_{0.95}\text{O}$ ) shows a similar broad Raman band<sup>[11,39]</sup> at  $643\text{ cm}^{-1}$ . However, the SEM spectra indicate that the content of Fe in these specimens is lower than the content of Mn. For all these reasons, the assignment of this band is not conclusive. Another common spectrum from the specimens 1, 2 and 6, Fig. 1A(b), would support the presence of bixbyite<sup>[22,24,29]</sup> in this black paint. Calcite has been identified in these specimens as well, Fig. 1A(b) and 1B(c). Haematite has also been discovered as another minor component, Fig. 1B(d), and amorphous carbon appears as the most abundant phase in the paint, Fig. 1B(e). Carbon atoms from amorphous carbon and carbonates have also been detected by XPS in these specimens, Figs S25 and S26 (Supporting information). These results suggest the use of a pictorial recipe with several components to prepare black paint. Amorphous carbon, Fig. S27b (Supporting Information), is also the dominant phase of the black paint used in other orthostat of this chamber, specimen 5, Fig. S6 (Supporting information). The micromorphology of the particles of this specimen reveals the presence of charcoal

microparticles, Fig. S28 (Supporting information). On the other hand, the main component of the red paint observed in the area of the specimens 3 and 4 is haematite, Figs S6 and S27a (Supporting Information). Secondary phases of gypsum, amorphous carbon and calcite have also been detected in this paint, Figs S27c and S27d (Supporting Information), indicating that a pictorial recipe was also used to elaborate the red paint. As stated previously, the basic components of the orthostats of the chamber H of the tumulus contain  $\alpha$ -quartz, albite<sup>[40]</sup> and muscovite. Nevertheless, phlogopite<sup>[41,42]</sup> and beryl,<sup>[43,44]</sup> two frequent minerals in granitic rocks, have also been detected in the specimen 3, Fig. 2(a, b, d, e, f) and Table 1.

A sinusoidal spectral profile is often observed in the  $\mu$ -RS spectra of particles producing an intense spectral background of fluorescence radiation,<sup>[12,20,45–47]</sup> Fig. 3a. This sinusoidal profile appears as a characteristic spectral pattern of the Raman microscope used. Therefore, a correction of this spectral artefact is possible. The  $\mu$ -RS spectrum of white light may be used (M. A. Ziemann, Universität Potsdam, Institut für Erd- und Umweltwissenschaften, Potsdam, Germany, personal communication, September 3, 2013), Fig. 3b, applying the appropriated baseline and subtraction procedures, Fig. 3c. Most of the spectra showing the indicated spectral background have been corrected by this method. Interferences of the fluorescence radiation in the Raman microscope are the probable origin of the observed sinusoidal signals. Thus, the  $\mu$ -RS spectrum of a polychromatic radiation like the white light can be used to obtain a reference pattern of these signals.

Some surprising materials have been discovered in the specimens 2, 3 and 6, Fig. 4. Microparticles of the synthetic polymer polystyrene have been detected in the specimen 3, Fig. 4a. A saturated

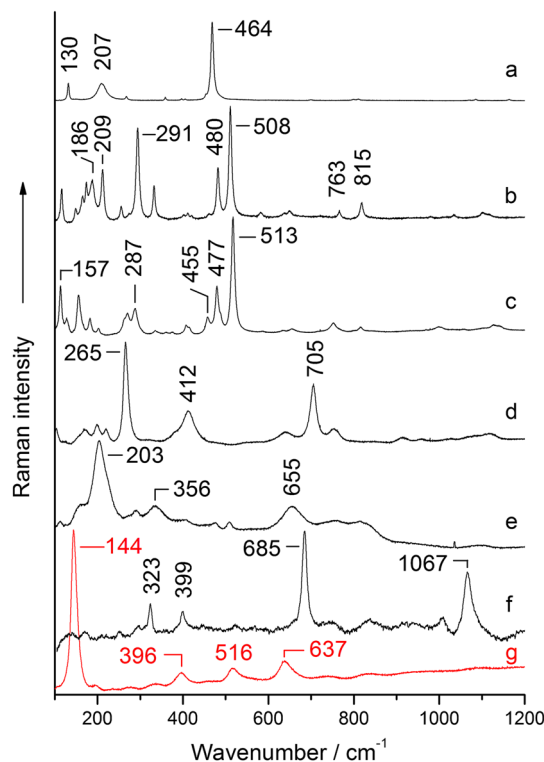


**Figure 2.** Representative micro-Raman spectroscopy spectra of components of the granitic orthostats with pictorial decorations in the megalithic monuments of Barnenez, Mont-Saint-Michel, Dissignac, Mané Rutual, Mané Kerioned B, gallery of Goërem and Bury stela: a,  $\alpha$ -quartz; b, low albite; c, microcline; d, muscovite; e, phlogopite; f, beryl; g, anatase.

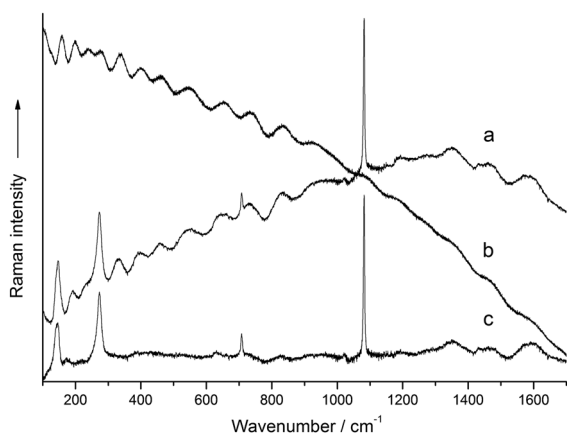


**Figure 3.** (a, b) Micro-Raman spectroscopy spectra recorded with the laboratory Raman microscope Jobin Yvon LabRam-IR HR-800 using 100 $\times$  magnification and the laser line at 632.8 nm. (a) Raw spectrum of calcite from the specimen 2 of black paint from the chamber H of Barnenez tumulus. (b) Spectrum of the white light from a halogen cold light source (Euromex LE.5210) with a maximum colour temperature at 3100 K. (c) Spectrum obtained after baseline and sinusoidal background corrections.

organic compound with Raman bands of methyl groups and C-C skeletal vibrations of linear chains is present in the specimen 2. The corresponding spectrum, Fig. 4b, has not yet been assigned to any common natural or synthetic compound. Finally, some blueish microparticles containing the synthetic polymorphic pigment copper-phthalocyanine blue<sup>[48–50]</sup> have been observed in the specimen 6, Fig. 4c. The intensity ratio between the bands at 484 and 172 cm<sup>-1</sup> indicates that the pigment corresponds to the crystalline structure of  $\epsilon$ -copper-phthalocyanine blue.<sup>[51]</sup> Polystyrene and copper-phthalocyanine were first produced about 1931 and 1935, respectively. These organic compounds could be considered as contamination from an external source, such as a marker pen and tracing materials. The chambers of this tumulus were discovered in the 1950s. The first tracings and photographs of the paintings of the chamber H were done on 1956 and 1958,

respectively.<sup>[4,17]</sup> A second series of tracings and photographs were obtained on 1968.<sup>[4]</sup> After that, direct tracings using transparent films and felt-tipped pens were made between 1968 and 1971. Since then, the chamber remained closed until restoration and research works were carried out last year. As a strict protocol to avoid contamination in the scission and handling of the specimens has been followed,<sup>[52,53]</sup> the presence of these materials in the paints could be attributed to inappropriate tracing techniques over the painted surfaces.

Intense spectral background of fluorescence radiation dominates the *in situ*  $\mu$ -RS spectra of a series of pictographs in this chamber, Fig. S6 (Supporting Information). Nevertheless, these spectra confirmed that  $\alpha$ -quartz and albite are components of the painted rocks. Characteristic spectral features in the region 1000–1500 cm<sup>-1</sup>, Fig. 5h, appear in numerous spectra. These features and the associated fluorescence emission could be related to colonies of fungi living on the surface of the rocks,<sup>[54–56]</sup> Fig. S29A (Supporting Information). The intense spectral background of the  $\mu$ -RS collected *in situ* makes difficult to identify Raman bands from the pigments.

Several pictographs may be observed on the orthostat of the entrance to the chamber A, Figs S4 and S7 (Supporting Information). The  $\mu$ -RS spectra of specimens of paint extracted from locations 1 and 2, Fig. S7 (Supporting Information), revealed the presence of goethite in both locations, Fig. 5a, and traces of haematite in the location 1, Table 1.

### Gallery of Goërem

The black pictographs of the P2 orthostat in the gallery of Goërem that have been studied in this work, Figs S9 and S10 (Supporting Information), were made using amorphous carbon as pigment, Fig. 5d and Table 1. The  $\mu$ -RS spectra of the extracted micro-specimens also indicate that besides  $\alpha$ -quartz, albite and muscovite, the granitic orthostat contains anatase, Fig. 3g. The contents in Na and K of the specimen 2 obtained by XPS, Table S1 (Supporting Information), would be due to the proximity of the gallery to the Atlantic Ocean.

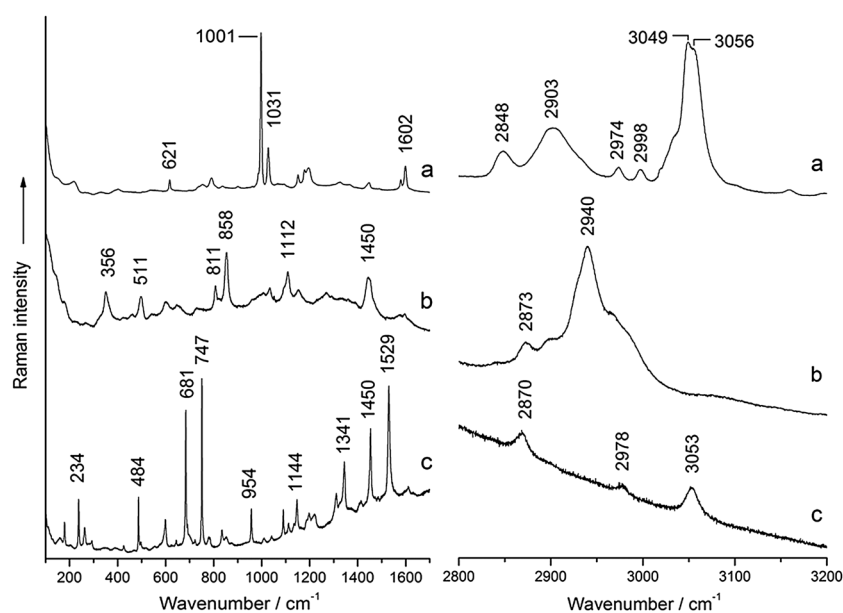


**Figure 4.** Representative micro-Raman spectroscopy spectra of contaminants present in the specimens of paints from the chamber H of Barnenez tumulus: (a) polystyrene, specimen 3; (b) saturated organic compound, specimen 2; (c)  $\epsilon$ -copper-phthalocyanine blue, specimen 6.

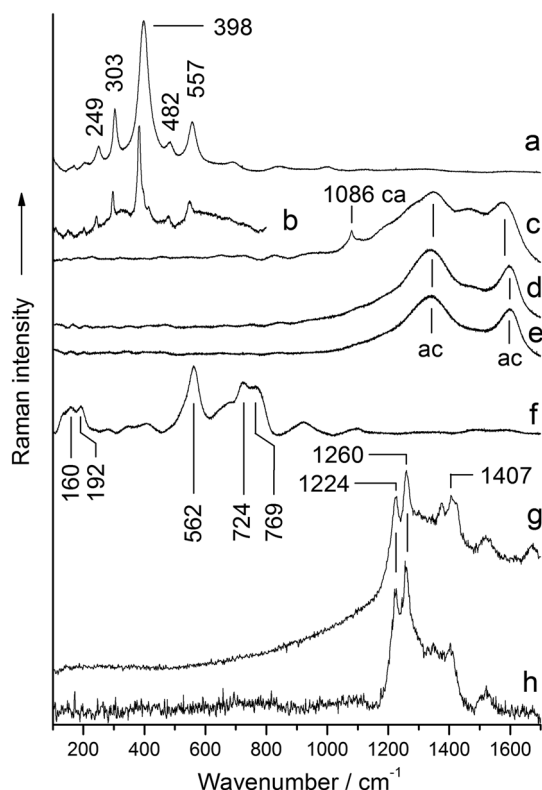


**Figure 5.** Representative micro-Raman spectroscopy spectra of: a, goethite from the paint specimen 2 of the Barnenez tumulus (chamber A); b, goethite from the paint specimen 2 of the L'Hirondelle stela; c, amorphous carbon from paint specimens of the Bury stela with traces of calcite; d, amorphous carbon from paint specimens 1–4 of the gallery of Goërem; e, amorphous carbon from paint specimens of the dolmens 2 and 3 of the Mont-Saint-Michel tumulus; f, celadonite from granitic rocks of the Mont-Saint-Michel tumulus. Representative *in situ* micro-Raman spectroscopy spectra of fungi covering the paintings of the (g) Dissignac and (h) Barnenez (chamber H) tumuli.

### Mont-Saint-Michel tumulus

Remains of painted decorations on orthostats of three dolmens of this tumulus have been studied, Figs S11–S17 (Supporting Information). The  $\mu$ -RS spectra of the specimen of red paint removed from the orthostat located in the ceiling of the chamber of the dolmen 1 show that haematite was used as pigment, Figs S11, S12 and S30d (Supporting Information). Amorphous carbon was used in the black paint of the dolmen 2 as well as in the specimens 1–4 of paints from the dolmen 3, Fig. 5e and Figs S14–S17 (Supporting Information). Nevertheless, haematite was mixed with amorphous carbon to prepare the paint used in the location of the specimen 2 from the dolmen 3, Figs S30b and S16 (Supporting Information). In addition to the usual rock components  $\alpha$ -quartz, albite and muscovite, green particles with layer structure have been detected in the orthostats of the three dolmens. The micas celadonite and muscovite form a mixed-layer join system generally described as solid solutions<sup>[57–59]</sup> that could account for the broad Raman bands observed in the spectra of these green particles, Fig. 5f. Colonies of fungi over the painted areas of the orthostats have made difficult to obtain *in situ*  $\mu$ -RS spectra of the pictorial materials, Figs S16 and S29BC (Supporting Information). Intense fluorescence emission from these colonies masks the Raman signals from the paint components. Raman bands of the fungi comparable with those obtained in the Barnenez and Dissignac tumulus, Fig. 5, and peaks of  $\alpha$ -quartz are hardly discernible from the spectral background.

### Dissignac tumulus

An analogous situation has been found in the *in situ*  $\mu$ -RS study of Dissignac tumulus, Figs S18 and S19 (Supporting Information). Spectral profiles similar to those obtained in the chamber H of Barnenez have been obtained from all the points of the orthostat with apparent traces of paint in the carvings. Raman bands of the fungi dominate the spectra, Fig. 5g, and very weak bands of  $\alpha$ -quartz are sometimes distinguishable.

### Mané Rutual dolmen

Despite aggressions suffered by this open monument, some traces of red paint are still evident inside. The  $\mu$ -RS spectra of a specimen of red paint extracted from one of these traces, Fig. S20 (Supporting Information), have shown that its main component is haematite, Fig. S30c, a common pigment used in prehistoric decorations. Very weak signals of  $\alpha$ -quartz from the rocky substratum appear in these spectra.

### Mané Kerioned B dolmen

Traces of red paint may also be perceived in the carvings of some orthostats of the Mané Kerioned B dolmen. A specimen of red paint, Fig. S21 (Supporting Information), has been analysed by  $\mu$ -RS and besides spectra of the usual components of the granitic substratum, Table 1, Raman bands of haematite and amorphous carbon, Fig. S30e (Supporting Information), are also shown in the spectra of the paint. As in the case of a pictograph of the dolmen 3 in the Mont-Saint-Michel tumulus, a pictorial recipe mixing haematite and amorphous carbon was used to elaborate the paint.

### L'Hirondelle stela

The stela from the megalithic quarry of L'Hirondelle has different areas painted in red and yellow, Fig. S22 (Supporting Information). A  $\mu$ -RS study of micro-specimens of these areas has shown that the red and yellow pigments used are respectively haematite and goethite, Fig. S30f (Supporting Information) and Fig. 5b, respectively. Very weak bands of amorphous carbon have also been detected. The stela was made from a dolomitic rock with some content of calcite, Table 1 and Fig. S31 (Supporting Information).

### Bury stela

Traces of pigments have been observed in this Neolithic stela. Several micro-specimens of them have been extracted. Their  $\mu$ -RS spectra have demonstrated that amorphous carbon mixed with calcite was used in the black traces of paint corresponding to the locations of the specimens 2 and 4, Fig. 5c, and haematite in the red trace corresponding to specimen 3, Figs S23 and S30a (Supporting Information). Abundant particles of  $\alpha$ -quartz and some of microcline, Fig. 2c, and anatase have also been detected in these specimens. Minerals that would come from rock used to make the stela.

Representative Raman spectra and signatures of haematite from the different monuments and stelae are collected in Fig. S30 (Supporting Information) and Table 2, respectively. Significant changes of relative intensity and full width at half height of some Raman bands are observed, particularly relevant are the changes of the bands at about 406 and 662  $\text{cm}^{-1}$ . The observed broadening of the band at  $\sim 406 \text{ cm}^{-1}$  with respect to full width at half height of this band in the Bury stela, Table 2, indicates that while well-crystallised

**Table 2.** Representative Raman signatures of haematite from different megalithic monuments and stelae

Paint micro-specimen								
BTH	BTH	BTA	MSMT 1	MSMT 3	MRD	MKDB	HS	BS
1, 2, 6	3, 4	1	1	2	1	1	1	3
220 vs	224 s	217 s	230 vw	230 m	226 m	221 m	215 s	229 vs
287 vs	289 s	280 vs	300 s	299 vs	291 vs	291 s	281 vs	295 s
402 m	401 m	396 m	414 s	414 m	404 m	406 vs	394 m	412 w
<b>(22)</b>	<b>(33)</b>	<b>(31)</b>	<b>(21)</b>	<b>(31)</b>	<b>(35)</b>	<b>(25)</b>	<b>(30)</b>	<b>(16)</b>
607 m	607 m	600 m	620 m	620 m	607 w	612 m	600 sh	613 w
651 m	657 m	656 m	667 vs	673 m	664 w	658 s	651 vs	662 w
1315 s	1303 vs	1308 s	1329 s	1337 m	1315 s	1330 m	1301 vs	1315 m

BTH, Barnenez tumulus, chamber H; BTA, Barnenez tumulus, chamber A; MSMT 1, Mont-Saint-Michel tumulus, dolmen 1; MSMT 3, Mont-Saint-Michel tumulus, dolmen 3; MRD, Mané Rutual dolmen; MKDB, Mané Kerioned B dolmen; HS, L'Hirondelle stela; BS, Bury stela; vs, very strong; s, strong; m, medium; w, weak; sh, shoulder.

Peaks observed in  $\text{cm}^{-1}$ . Wavenumbers between parentheses are the full width at half height of the previous Raman band.

It is the way to indicate the relevance of this parameter (full width at half height for the band around  $400 \text{ cm}^{-1}$ ) in order to estimate the crystallinity of the haematite used as pigment.

haematite was used in this stela, structural disordered haematite was used in the other cases.<sup>[6]</sup> The increase of relative intensity of the band at  $\sim 662 \text{ cm}^{-1}$  respect to the band at  $\sim 610 \text{ cm}^{-1}$  is an additional indication of the presence of disordered crystal structures of haematite. The band at  $610 \text{ cm}^{-1}$  is assigned to a Raman active  $E_g$  phonon,<sup>[60,61]</sup> whereas the band at  $\sim 662 \text{ cm}^{-1}$  is assigned to an infrared active longitudinal optical  $E_u$  mode, observable in Raman because of the change of symmetry in disordered structures.<sup>[9,11,62]</sup>

## Conclusions

The  $\mu$ -RS studies of micro-specimens of traces of paintings from a significant group French megalithic monuments and stelae have revealed the use of typical prehistoric pigments like haematite, goethite, amorphous carbon and manganese oxides/oxihydroxides. Pictorial recipes to prepare the paint by mixing some of these pigments and adding calcite and gypsum have been detected in a number of cases. Additional *in situ*  $\mu$ -RS studies using a portable Raman microscope have faced a difficult problem, colonies of fungi living over the paintings in closed chambers of the monuments. Intense fluorescence emission and Raman bands from the fungi masked the bands from the pictorial materials. Only bands from the rock components have been able to detect in several cases. The presence of these colonies over paintings containing amorphous carbon poses a serious problem to obtain reliable radiocarbon dates of these paintings. The SEM/EDX and XPS complimentary techniques have contributed to interpret the  $\mu$ -RS spectra. Several particles of organic compounds, some of them of modern synthetic origin (polystyrene and  $\epsilon$ -copper-phthalocyanine blue), have been detected in a pictograph from Barnenez tumulus. They would be the result of an external contamination, possibly by the use of inappropriate tracing techniques. Well-crystallised haematite has been detected in the red paintings of the Bury stela. However, haematite with disordered structures was used in the paintings from the other sites. The sinusoidal spectral pattern from the fluorescence emission background has been properly corrected using the  $\mu$ -RS spectrum of white light. Pictorial decoration appears as a frequent practice in French megalithism. The pigment specimens studied here are the first to be documented within the megalithic contexts

from northwestern France. The red, yellow and black paintings, and fillers inside the engravings, are considerably appealing to understand systematic techniques and themes already broadly documented with similar chronologies in the Iberian Peninsula,<sup>[1,4]</sup> and thereby to understand late prehistory rituals around Europe.

## Acknowledgements

We thank Dr S. Martin (UNED) for his help in recording SEM/EDX data. This work presents results from the Colours of Death research project HAR2012-34709 of the Spanish Ministerio de Economía y Competitividad and the Barnenez, Plouezoc'h, Finistère research project supported by the Direction Régionale des Affaires Culturelles de Bretagne and its Regional Archaeological Service. Financial support from the European Regional Development Fund (ERDF) is also gratefully acknowledged. Three referees and the Editor Philippe Colomban offered comments that improved the manuscript.

## References

- [1] P. Bueno Ramírez, R. de Balbín Behrmann, R. Barroso Bermejo, *L'Anthropologie* **2007**, *111*, 590.
- [2] F. Carrera Ramírez, *El arte parietal en monumentos megalíticos del Noroeste ibérico. Valoración, diagnosis y conservación*, British Archaeological Reports International series S2190, Archaeopress, Oxford, UK, **2011**.
- [3] P. Bueno Ramírez, R. de Balbín Behrmann, *Anthropologie* **2002**, *106*, 603.
- [4] P. Bueno Ramírez, R. de Balbín Behrmann, L. Laporte, P. Gouezin, F. Cousseau, R. Barroso, A. Hernanz, M. Iriarte, L. Quesnel, *Antiquity* **2015**, *89*, 55.
- [5] H. G. M. Edwards, E. M. Newton, J. Russ, *J. Mol. Struct.* **2000**, *550–551*, 245.
- [6] F. Ospitali, D. C. Smith, M. Lorblanchet, *J. Raman Spectrosc.* **2006**, *37*, 1063.
- [7] A. Hernanz, J. M. Gavira-Vallejo, J. F. Ruiz-López, H. G. M. Edwards, *J. Raman Spectrosc.* **2008**, *39*, 972.
- [8] A. Tournié, L. C. Prinsloo, C. Paris, P. Colomban, B. Smith, *J. Raman Spectrosc.* **2011**, *42*, 399.
- [9] C. Lofrumento, M. Ricci, L. Bachechi, D. De Feod, E. M. Castellucci, *J. Raman Spectrosc.* **2012**, *43*, 809.
- [10] S. Lahlii, M. Lebon, L. Beck, H. Rousselière, C. Vignaud, I. Reiche, M. Menu, P. Paillet, F. Plassard, *J. Raman Spectrosc.* **2012**, *43*, 1637.

- [11] A. Hernanz, J. M. Gavira-Vallejo, J. F. Ruiz-López, S. Martín, Á. Maroto-Valiente, R. de Balbín-Behrmann, M. Menéndez, J. J. Alcolea-González, *J. Raman Spectrosc.* **2012**, *43*, 1644.
- [12] A. Hernanz, J. F. Ruiz-López, J. M. Madariaga, E. Gavrilenko, M. Maguregui, S. Fdez-Ortiz de Vallejuelo, I. Martínez-Arkarazo, R. Alloza-Izquierdo, V. Baldellou-Martínez, R. Viñas-Vallverdú, A. Rubio i Mora, Á. Pitarch, A. Giakoumaki, *J. Raman Spectrosc.* **2014**, *45*, 1236.
- [13] T. R. Ravindran, A. K. Arora, M. Singh, S. B. Ota, *J. Raman Spectrosc.* **2013**, *44*, 108.
- [14] J. F. Ruiz, M. Mas, A. Hernanz, M. W. Rowe, K. L. Steelman, J. M. Gavira, *Int. Newsl. Rock Art (INORA)* **2006**, *46*, 1.
- [15] J. F. Ruiz-López, A. Hernanz, R. A. Armitage, R. Viñas-Vallverdú, J. M. Gavira-Vallejo, M. W. Rowe, A. Rubio i Mora, *J. Archaeol. Sci.* **2012**, *39*, 2655.
- [16] P. Bueno Ramírez, R. de Balbín Behrmann, L. Laporte, P. Gouezin, R. Barroso Bermejo, A. Hernanz Gismero, J. M. Gavira-Vallejo, M. Iriarte Cela, *Trabajos de Prehistoria* **2012**, *69*, 123.
- [17] P. R. Giot, *Bamenez, Guenno, Carn*, Travaux du Laboratoire d'Anthropologie – Préhistoire Protohistoire Quaternaire armoricains, Université du Rennes I, Rennes, France, **1987**.
- [18] G. Benéteau-Douillard, *Le complexe mégalithique du Bois de Fourgon à Avrillé (Vendée). Etudes archéologiques et techniques d'un ensemble de menhirs et stèles anthropomorphes en Centre-Ouest Atlantique*, Groupement Vendéen de Sauvegarde du Patrimoine Archéologique, La Roche Sur Yon, France, **2012**.
- [19] L. Salanova, M. Sohn, in *Le bois dans l'aménagement de la tombe: quelques approches?* (Eds: F. Carré, F. Henrion), *Mémoires de l'Association Française d'Archéologie Mérovingienne (AFAM)* vol. XXIII, Saint-Germain-en-Laye, France, **2012** p. 221–228.
- [20] A. Hernanz, J. F. Ruiz-López, J. M. Gavira-Vallejo, S. Martín, E. Gavrilenko, *J. Raman Spectrosc.* **2010**, *41*, 1394.
- [21] A.S.T.M. Subcommittee on Raman Spectroscopy, *Raman Shift Frequency Standards: McCreery Group Summary (ASTM E 1840)*. American Society for Testing Materials: Philadelphia, PA, **2015**. <http://www.chem.ualberta.ca/~mccreery/raman.html>.
- [22] F. Buciuman, F. Patras, C. Radu, D. R. T. Zahn, *Phys. Chem. Chem. Phys.* **1999**, *1*, 185.
- [23] C. M. Julien, M. Massot, R. Baddour-Hadjean, S. Frenger, S. Bach, J. P. Pereira-Ramos, *Solid State Ion.* **2003**, *159*, 345.
- [24] C. M. Julien, M. Massot, C. Poinsignon, *Spectrochim. Acta A* **2004**, *60*, 689.
- [25] H.-S. Kim, P. C. Stair, *J. Phys. Chem. B* **2004**, *108*, 17019.
- [26] H. Y. Xu, S. L. Xu, X. D. Li, H. Wang, H. Yan, *Appl. Surf. Sci.* **2006**, *252*, 4091.
- [27] L.-X. Yang, Y.-J. Zhu, H. Tong, W.-W. Wang, G.-F. Cheng, *J. Solid State Chem.* **2006**, *179*, 1225.
- [28] N. Mironova-Ulmanea, A. Kuzmina, M. Grubeb, *J. Alloys Compd.* **2009**, *480*, 97.
- [29] S.-H. Shim, D. LaBounty, T. S. Duffy, *Phys. Chem. Minerals* **2011**, *38*, 685.
- [30] Z.-Y. Tian, P. M. Kouotou, N. Bahlawane, P. H. T. Ngamou, *J. Phys. Chem. C* **2013**, *117*, 6218.
- [31] D. C. Smith, M. Bouchard, M. Lorblanchet, *J. Raman Spectrosc.* **1999**, *30*, 347.
- [32] A. Zoppi, G. F. Signorini, F. Lucarelli, L. Bachechi, *J. Cult. Herit.* **2002**, *3*, 299.
- [33] A. Pitarch, J. F. Ruiz, S. Fdez-Ortiz de Vallejuelo, A. Hernanz, M. Maguregui, J. M. Madariaga, *Anal. Methods* **2014**, *6*, 6641.
- [34] F. Froment, A. Tournié, P. Colombari, *J. Raman Spectrosc.* **2008**, *39*, 560.
- [35] M. C. Bernard, A. Hugot-Le Goff, B. Vu Thi, S. Cordoba de Torresi, *J. Electrochem. Soc.* **1993**, *140*, 3065.
- [36] J. Zuo, C. Xu, Y. Liu, Y. Qian, *Nanostruct. Mater.* **1998**, *10*, 1331.
- [37] P. Jezequel, G. Wille, C. Bery, F. Delorme, V. Jean-Prost, R. Cottier, J. Breton, F. Dure, J. Despré, *J. Archaeol. Sci.* **2011**, *38*, 1165.
- [38] R. T. Downs, The RRUFF Project, 19th General Meeting of the International Mineralogical Association, Kobe, Japan, **2006**, O03–13, 117.
- [39] D. L. A. de Faria, S. Venâncio Silva, M. T. de Oliveira, *J. Raman Spectrosc.* **1997**, *28*, 873.
- [40] J. J. Freeman, A. Wang, K. E. Kuebler, B. L. Jolliff, L. A. Haskin, *Can. Mineral.* **2008**, *46*, 1477.
- [41] A. Tlili, D. C. Smith, J.-M. Beny, H. Boyer, *Mineral. Mag.* **1989**, *53*, 165.
- [42] D. A. McKeown, M. I. Bell, E. S. Etz, *Am. Mineral.* **1999**, *84*, 970.
- [43] O. F. Mets, *Int. Geol. Rev.* **1975**, *17*, 382.
- [44] P. Uher, P. Chudík, P. Bačík, T. Vaculovič, M. Galiová, *J. Geosci.* **2010**, *55*, 69.
- [45] T. R. Ravindran, A. K. Arora, M. Singh, S. B. Ota, *J. Raman Spectrosc.* **2013**, *44*, 108.
- [46] M. Iriarte, A. Hernanz, J. F. Ruiz-López, S. Martín, *J. Raman Spectrosc.* **2013**, *44*, 1557.
- [47] H. Gomes, H. Collado, A. Martins, G. H. Nash, P. Rosina, C. Vaccaro, L. Volpe, *Mediterr. Archaeol. Ar.* **2015**, *15*, 163.
- [48] L. I. McCann, K. Trentelman, T. Possley, B. Golding, *J. Raman Spectrosc.* **1999**, *30*, 121.
- [49] L. Burgio, R. J. H. Clark, *Spectrochim. Acta Part A* **2001**, *57*, 1491.
- [50] T. D. Chaplin, R. J. H. Clark, A. McKay, S. Pugh, *J. Raman Spectrosc.* **2006**, *37*, 865.
- [51] C. Defeyt, P. Vandenabeele, B. Gilbert, J. Van Pevenage, R. Clootse, D. Strivaya, *J. Raman Spectrosc.* **2012**, *43*, 1772.
- [52] A. Hernanz, M. Mas, B. Gavilán, B. Hernández, *J. Raman Spectrosc.* **2006**, *37*, 492.
- [53] A. Hernanz, J. M. Gavira-Vallejo, J. F. Ruiz-López, *J. Raman Spectrosc.* **2006**, *37*, 1054.
- [54] H. G. M. Edwards, N. C. Russell, R. Weinstein, D. D. Wynn-Williams, *J. Raman Spectrosc.* **1995**, *26*, 911.
- [55] S. Ghosal, J. M. Macher, K. Ahmed, *Environ. Sci. Technol.* **2012**, *46*, 6088.
- [56] K. D. Gussemma, P. Vandenabeele, A. Verbeken, L. Moens, *Spectrochim. Acta Part A* **2005**, *61*, 2896.
- [57] V. Velde, *Contrib. Mineral. Petr.* **1972**, *77*, 235.
- [58] G. Monier, J.-L. Robert, *Mineral. Mag.* **1986**, *50*, 257.
- [59] L. M. Keller, C. de Capitani, R. Abart, *J. Petrol.* **2005**, *46*, 2129.
- [60] I. Chamritski, G. J. Burns, *Phys. Chem. B* **2005**, *109*, 4965.
- [61] D. Bersani, P. P. Lottici, A. Montenero, *J. Raman Spectrosc.* **1999**, *30*, 355.
- [62] A. M. Jubb, H. C. Allen, *ACS Appl. Mater. Interfaces* **2010**, *2*, 2804.

## Supporting information

Additional supporting information may be found in the online version of this article at the publisher's web site.